Tellus (2000), 52B, 652–661
Printed in UK. All rights reserved

TELLUS
ISSN 0280–6509

ACE-2 multiple angle micro-pulse lidar observations from Las Galletas, Tenerife, Canary Islands

By DONNA M. POWELL[1]*, JOHN A. REAGAN[1], MANUEL A. RUBIO[1], WAYNE H. ERXLEBEN[1] and JAMES D. SPINHIRNE[2], [1]*University of Arizona, Tucson, AZ, 85721, USA;* [2]*NASA Goddard Space Flight Center, Greenbelt, MD 20771, USA*

(Manuscript received 17 February 1999; in final form 22 September 1999)

ABSTRACT

Multiple-angle micro-pulse lidar (MPL) observations were made at Las Galletas on Tenerife, Canary Islands during the Aerosol Characterization Experiment-2 (ACE-2) conducted June–July, 1997. A principal objective of the MPL observations was to characterize the temporal/spatial distributions of aerosols in the region, particularly to identify and profile elevated Saharan dust layers which occur intermittently during the June–July time period. Vertical and slant angle measurements taken 16 and 17 July characterize such an occurrence, providing aerosol backscatter, extinction, and optical depth profiles of the dust layer between 1 and 5 km above mean sea level (MSL). Additionally, horizontal measurements taken in Las Galletas throughout the 6-week period provide a time profile of the varying aerosol extinction at the surface. This profile exhibits the alternating periods of clean maritime air and pollution outbreaks that typified the region. Horizontal measurements also provide some evidence suggesting the possible influx of Saharan dust from the free troposphere to the surface. This paper presents estimates of aerosol optical properties retrieved from the multi-angle MPL measurements in addition to an outline of the methodologies employed to obtain these results.

1. Introduction

Micro-pulse lidar (MPL) observations were made at Las Galletas on Tenerife, Canary Islands June and July, 1997 as part of the Aerosol Characterization Experiment-2 (ACE-2). ACE-2 was a continued extensive international effort to study and measure the optical and radiative properties of aerosols from European and African sources (Raes et al., 2000). The inclusion of MPL observations at Las Galletas as a part of ACE-2 came rather late in planning for the experiment fostered by an identified need for added sensing capabilities to discern the presence and radiative effects of Saharan dust episodes that occur in the North Atlantic region during the summer season. These dust events are a result of strong convective disturbances in West Africa and entail the passage of an elevated layer of dust, typically at an altitude between one and five kilometers above MSL (Karyampudi and Carlson, 1988); further validation and characterization of Saharan dust events, enabled by analysis of shuttle lidar data obtained during the LITE mission, has recently been reported by Karyampudi et al. (1999). An example of an apparent dust episode occurred on the evening of 16 July with a dust layer that persisted well through 17 July. Aerosol optical properties of this dust layer were retrieved during this time-period from MPL measurements made in the vertical and at various slant angles. These properties include aerosol backscatter, extinction, and optical depth. Algorithms used to derive these results included slant-sensing techniques

* Corresponding author: University of Arizona, Bldg. 104, Tucson, AZ, 85721, USA.
e-mail: dpowell@ece.arizona.edu.

(Spinhirne et al., 1980; Reagan et al., 1984), and a two-scatterer formulation based on Fernald et al. (1972). The retrieval methods employed did not rely on the use of auxiliary measurements. However, co-located daytime solar radiometer measurements taken during the cloud-free periods of the dust event provided estimates of total aerosol optical depth which could be compared to the MPL results. The principal objectives of the ACE-2 Las Galletas MPL observations, the results of which are reported here, were 2-fold:

- To detect the presence and vertical structure of significant aerosol events, particularly Saharan dust events.
- To demonstrate that an MPL could be employed in the quantitative retrieval of aerosol optical properties via slant angle and horizontal sensing in addition to conventional vertical soundings.

The site of the MPL measurements, Las Galletas, is located at the Southern tip of Tenerife in the Costa del Silencio region (28°0′N, 16°39′W) at approximately MSL. The ACE-2 project involved concurrent instrument measurements made at several other locations on Tenerife. The 16 and 17 July dust episode offered an opportunity for a comparative study of aerosol optical properties retrieved at the different sites. In particular, results obtained from the Las Galletas MPL could be compared with those from a second MPL located at the Izana Observatory (IZO), a weather station near the center of Tenerife (28°30′N, 16°50′W) at an altitude of 2360 m above MSL (Welton et al., 2000), and with measurements from an airborne sunphotometer (Schmid et al., 2000).

Horizontal, near surface MPL measurements were also made at Las Galletas throughout the six-weeks of ACE-2. It is not possible to make such measurements in an unrestricted area with conventional visible wavelength lidar due to eye-safety concerns, but doing so is not a problem with the eye-safe MPL design that was operated at Las Galletas. Aerosol extinction estimates were retrieved from the horizontal MPL measurements by application of the slope method technique (Collis, 1966). These results provide a time profile of the varying values of extinction at the surface and in particular exhibit the alternating periods of maritime clean air and pollution outbreaks that occurred in the North-East Atlantic region during the measurement period. Additionally, the horizontal measurements provided a chance to observe any correlation between increased aerosol extinction at the surface and the passage of an upper level dust layer. Such a correlation would suggest the infiltration of aerosol from the dust layer through the Marine Boundary Layer (MBL). As presented later in this paper, vertical and horizontal MPL measurements taken during and one day subsequent to the passage of the elevated dust layer, on 18 July, appear to support this idea.

2. Instrumentation

2.1. Micro-pulse lidar

The MPL used for the ACE-2 observations is a compact ground-based aerosol and cloud profilometer based on recent advances of laser and detector technology applicable for a lidar system. These systems employ a pulsed frequency-doubled Nd:YLF laser (2.5 kHz with 10 μJ/pulse at 523 nm), a 20 cm telescope as dual transmitter/receiver, narrow-bandwidth optical filters (effective bandpass 0.18 nm FWHM), narrow detector field of view, and a high quantum efficiency single-photon counting APD detector. Laser eye-safety is achieved through volume expansion of a rapidly pulsed low-power beam by the telescope transmitter/receiver. Range resolution is as fine as 30 m with ranging distances out to 30 km. Data are normally time averaged in 1-minute intervals, allowing high temporal resolution. Initial systems with 300-meter resolution, were developed at Goddard Space Flight Center (Spinhirne, 1993). Commercially available high-resolution systems are now being produced under a technology transfer/development agreement between NASA and Science & Engineering Services, Inc. (SESI). Systems have been successfully deployed at Department of Energy (DOE) Atmospheric Radiation Measurement (ARM) sites beginning in 1993 (Spinhirne et al., 1995) and have demonstrated full-time, long term operation capabilities.

The MPL was configured with an external moveable mirror to permit horizontal and slant-angle measurements in addition to the standard vertical profiling capabilities of the system. The mirror system consisted of a square 30.5 cm × 30.5 cm mirror mounted at a 45-degree angle on a rotating shaft. The shaft was rotated by a PC-controlled stepper motor that provided a turning angle resolution of 0.009 degrees. The MPL was positioned horizontally allowing the option to take horizontal measurements with or without the use of the external mirror.

2.2. *Solar radiometer*

The solar radiometer at the Las Galletas site was an automated, self-tracking system designed and built at the University of Arizona. Measurements were made at ten different spectral channels including 520 nm, which corresponded well with the 523 nm wavelength of the MPL system. The radiometer was operated concurrently with the MPL during daylight hours when significant cloud-free conditions prevailed. A complete description of this instrument and the procedures employed to retrieve optical depths is given by Ehsani et al. (1998).

3. Data acquisition and processing

3.1. *Data sampling*

The MPL data were collected with 75-m resolution and with a ranging distance out to 30 km. The pulse repetition frequency (PRF) of 2.5 kHz summed over a measurement interval of sixty seconds provides a total of 150,000 laser shots per accumulated backscatter profile. The data acquisition allowed the option to sample out to a range of 60 km to retrieve an estimate of the system background, but the primary data were only collected and recorded for 30 km. The MPL raw signals as collected and recorded consist of photoelectron counts per range bin.

The MPL was operated nearly continuously throughout ACE-2. All measurements, with the exception of some horizontal measurements, were implemented using the external mirror. Prevalently, the laser beam was oriented via the mirror in the vertical or at a slant of 45 or 48°. Periodic horizontal measurements were then taken, often on the hour, each for a duration of at least 15 min. Finally, at various times during each 24-h period, slant measurements were taken at three different angles (48, 60 and 70.5°) followed by a measurement made in the vertical. Successful slant-angle retrieval methods rely on temporal homogeneity; thus, measurements at each angle were only taken for a brief duration of time. A typical protocol for the slant-angle sampling consisted of 4, 5 and 8 min measurements taken for the corresponding angles 48, 60 and 70.5°.

3.2. *The Normalized Lidar Signal*

The normalized lidar return signal for one transmitted laser pulse of energy E_o(centered on a wavelength of 523 nm) can be expressed by

$$X(r) = \frac{[n(r) - n_{BD} - n_{Ap}(r)]r^2}{O(r)E_o} = C\beta(r)T^2(r), \qquad (1)$$

where $n(r)$ is the photoelectron count for backscattering from a range bin Δr centered at ranging distance r from the lidar, n_{BD} is the noise count due to background radiation, $n_{Ap}(r)$ is the afterpulse count of the photon detector, $O(r)$ is the overlap factor to correct for transmitter/receiver near-range field of view (FOV) conflicts, C is the calibration constant, $\beta(r)$ is the atmospheric unit volume backscattering coefficient, and $T^2(r)$ is the atmospheric round-trip transmittance. The unit volume extinction coefficient, $\sigma(r)$, is related to round-trip transmittance by

$$T^2(r) = \exp\left[-2\int \sigma(r')\,dr'\right]. \qquad (2)$$

The backscatter and extinction coefficients may be expressed as the sum of the Rayleigh and aerosol scattering components, given by

$$\sigma(r) = \sigma_R(r) + \sigma_a(r) \quad \text{and} \quad \beta(r) = \beta_R(r) + \beta_a(r), \qquad (3)$$

where subscripts denote Rayleigh and aerosol, respectively. The lidar signal may be expressed either in terms of the backscatter or extinction coefficient through the use of extinction to backscatter parameters, S_a and S_R, given by

$$S_R(r) = \frac{\sigma_{R(r)}}{\beta_R(r)} \quad \text{and} \quad S_a(r) = \frac{\sigma_{a(r)}}{\beta_a(r)}. \qquad (4)$$

The Rayleigh ratio has a constant value of $S_R(r) = 8\pi/3$, while S_a can take on a wide range of values depending on the aerosol size distribution and particle refractive index (Reagan et al., 1988).

3.3. Signal corrections

Achieving the normalized MPL signal given in eq. (1) requires the application of background, energy, range, afterpulse, and overlap corrections. Background and energy correction values are stored and collected by the MPL system and are easily applied to the raw signal for normalization. Applying a range correction requires an inspection of the raw signal to determine the lag time between when the system begins counting and when the laser actually started pulsing. The Tenerife MPL had a lag of approximately 450 ns, indicating that the first bin of each 400-bin profile should be ignored. The afterpulse correction is determined by attenuating the lidar-beam at near-ranges, for example, by directing the beam into thick cloud or at a hard target, and inspecting the resulting residual signal. This technique is described in detail in Campbell et al. (1998). The final correction applied to achieve the normalized lidar signal is an optical overlap correction. The method for deriving this correction is also described by Campbell et al. and is briefly outlined later in this paper. Separate overlap functions, $O(r)$ (see eq. (1)), must be determined for the MPL system both with and without the use of the external mirror. Optical properties of the mirror provide full overlap (an overlap factor of one) at a shorter distance than the non-mirror signal. The mirror and non-mirror signals were found to achieve full overlap at approximately 1.5 and 4.25 km respectively (Powell et al., 1998). The observed 16–17 July dust layer was typically well above 1.5 km and thus outside of the region affected by overlap correction uncertainty.

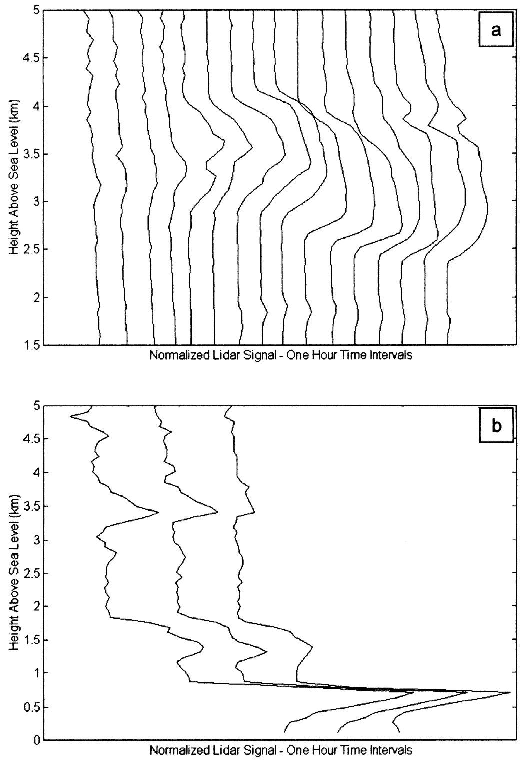

Fig. 1. MPL normalized lidar signal, 16-h time period during the 16 and 17 July Saharan dust episode (a) and subsequent 3-h period on 18 July (b). Each profile is a 20 min average at 1-h time intervals.

4. Results and analysis

4.1. 16 and 17 July dust episode

Mid-afternoon on 16 July, the first evidence of a Saharan dust was observed in the vertical MPL measurements taken in Las Galletas. The history of the event is illustrated in a series of normalized signal, $X(r)$, profiles plotted against vertical height above MSL (Fig. 1a). Each profile is an average of about 20 min of MPL vertical measurements at 1-hour time intervals. Beginning at 15 GMT, traces of aerosol structure were observed in the region between 3 and 4 km MSL, well above the top of the MBL. This structure steadily increased and by 20 GMT a well-formed elevated layer of dust prevailed. The layer signal continued to increase for the next several hours. Between 23 GMT on 16 July and 0 GMT on 17 July the entire dust layer essentially descended a quarter of a kilometer. The bottom of the dust layer continued to drop from a height of 2.6 km at 0 GMT to 2.3 km within the ensuing hours of that early morning. By 6 GMT, 15 h after the dust layer was first observed, the vertical extension of the layer had thickened to about 2 km. The strongest return signal for the dust layer observed by the Las Galletas MPL measurements occurred around 16 GMT on 17 July (outside the time range of Fig. 1a). Subsequent to this time the layer strength had begun to weaken. A second plot of measurements taken late on 18 July (Fig. 1b), analogous to the time profile shown in Fig. 1a, illustrates residual dust in a weak layer centered at approximately 3.5 km and what appears to be a second region of dust directly on top of the MBL.

4.1.1. Slant sensing retrieval. Slant-angle sensing is a retrieval technique implemented under the assumption of reasonable horizontal homogeneity. For measurements along a slant range r at angle θ from the zenith, $T^2(r)$ reduces to

$$T^2(r) = \exp[-2\tau(z) \sec \theta], \tag{5}$$

where $\tau(z)$ is the partial optical depth to vertical height z (i.e., $\sigma(z)$ integrated to height z). For measurements at several slant angles θ, a straight-line fit to $\ln[X(r)]$ versus $2 \sec \theta$, for data at a given height $z(r = z\sec \theta)$, yields a line of slope $-\tau(z)$ (Spinhirne et al., 1980). The aerosol component $\tau_a(z)$ can then be determined by subtracting the known Rayleigh component. The scatter of points around the straight-line fit reflects how well the assumption of horizontal homogeneity holds true.

Slant-angle measurements were taken the evening (21–22 GMT) of 17 July during the Saharan dust event. A plot of the slant-path signals normalized to equivalent vertical height above MSL is shown in Fig. 2. As mentioned previously, quantitative aerosol optical depth retrieval relies on reasonable atmospheric homogeneity in the horizontal. For the slant-path profiles, horizontally adjacent atmospheric structural features such as clouds or aerosol layers, and a progressively weaker signal at any given equivalent vertical height as the slant-path angle value increases, are good indications of homogeneity. Fig. 2 exhibits these qualities reasonably well, although the height differential between the vertical measurement and the other slant-measurements at 1 km suggests some possible inhomogeneity.

Examining the slant-angle profiles, the top of the marine boundary layer (MBL) is evident at approximately 1 km, and the dust layer can be seen between 1.5 and 5 km. Partial optical depth values retrieved for this dust event using the straight-line fitting methodology described earlier are presented in Table 1. The aerosol optical depth of the dust layer can be obtained from the difference of $\tau_a = 0.298$ (height 4.58 km) and $\tau_a = 0.127$ (height 1.5 km), which yields $\tau_a = 0.171$ with an uncertainty, estimated from the standard deviation of the straight-line fitting, of ± 0.02.

4.1.2. Vertical 2-scatterer retrieval. Retrieval of vertical backscatter and extinction profiles typically requires a general two type of scatterer solu-

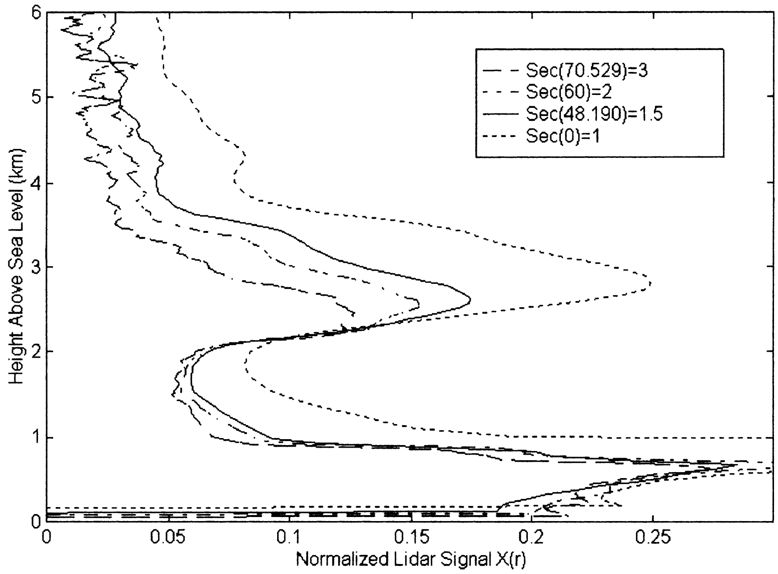

Fig. 2. Vertical and slant-angle measurements taken during Saharan dust episode 17 July, 21–22 GMT. The normalized signal $X(r)$ is in units of (PhE/μ) km^2.

Table 1. *Aerosol partial optical depth values retrieved from slant-path measurements for 17 July dust event at 21–22 GMT*

	Vertical height (km)	τ_a	Standard deviation
top of layer	4.58	0.298	0.0089
	3.30	0.284	0.0064
	3.23	0.274	0.0085
	3.15	0.279	0.0096
	3.08	0.265	0.0115
	3.00	0.269	0.0090
	2.93	0.257	0.0061
	2.85	0.239	0.0035
	2.78	0.195	0.0031
	2.70	0.153	0.0026
bottom of layer	1.50	0.127	0.0107

tion of the lidar equation (i.e., both molecular or Rayleigh scattering and aerosol scattering are important). Following the approach of Fernald et al. (1972) an analytic solution for $\beta_a(z)$ and $\sigma_a(z)$ may be obtained by requiring S_a to be constant with range over the height interval for which the solution is obtained. This constraint permits the aerosol number density to vary freely with range, but restricts the aerosol phase function to be constant. It is a reasonable assumption for well mixed atmospheric regions, particularly if the humidity isn't too high and doesn't change greatly with height. Implementation of this solution approach also requires determination of the lidar calibration constant C. As can be seen from eq. (1), C may be determined from $X(z_c)$ at some reference calibration height z_c if $T^2(z_c)$ and $\beta(z_c)$ are known. Slant path measurements can be used to obtain $T^2(z_c)$ and, by picking z_c in the clean free troposphere where $X(z)$ tracks the relative spatial variation expected for Rayleigh scattering, $\beta(z_c)$ can be expected to be well approximated as $\beta_R(z_c)$ within a few percent for the MPL wavelength (523 nm). The value of $\beta_R(z_c)$ may be calculated absolutely from Rayleigh scattering theory using an air number density at z_c determined from pressure/temperature values obtained from meteorological sounding data. Using vertical and slant-angle MPL measurements taken 17 July at about 22 GMT, an estimate of $C = 13.5 \pm 0.5$ was obtained from these measurements. The estimated uncertainty in C is mainly attributed to the uncertainty in $\tau(z_c)$ determined from the slant-angle observations.

Following determination of the calibration constant, the backscatter profile may be retrieved using a solution after Fernald et al. (1972) given by

$$\beta_a(z) + \beta_R(z) = \frac{X(z)\exp\left[-2(S_a - S_R)\int_{z_c}^{z}\beta_R(z)\,dz\right]}{CT^2(z_c) - 2S_a\left[\int_{z_c}^{z} X(z) \times \exp\left[-2(S_a - S_R)\int_{z_c}^{z}\beta_R(z')\,dz'\right]dz\right]}. \quad (6)$$

A value was first assumed for S_a, permitting determination of $\beta_a(z_c)$. Next, $\sigma_a(z)$, determined by $\sigma_a(z) = S_a\beta_a(z_c)$, was integrated over the dust layer thickness ($z = 1.5$ km to $z = 4.6$ km), thereby yielding the dust layer aerosol optical thickness τ_a, for the assumed value of S_a. This was repeated with different trial values of S_a to determine the S_a value that produced a τ_a in agreement with the slant-angle retrieval, $\tau_a = 0.171 \pm 0.02$. The solution thus obtained was $S_a(z) = 35 \pm 5$. Having determined the S_a value yielding the τ_a in best agreement with the 17 July, 21 GMT MPL slant-angle observations, estimates of the dust layer τ_a could then be obtained from vertical MPL data collected at other times based on the assumption that S_a remained fairly constant during the approximately 24 h period that the dust layer persisted over the Las Galletas MPL site.

Values for τ_a for the dust layer between 16 July, 20 GMT and 17 July, 22 GMT are presented in Fig. 3. The uncertainty in τ_a by the direct slant-angle retrieval method at 21 GMT, 17 July is only about 10%, but τ_a retrieved at other times based on only vertical MPL observations, via eq. (6) and $\tau_a(z) = S_a\beta_a(z)$, are inherently more uncertain (i.e., as reflected in the determination of $S_a = 35 \pm 5$ for $\tau_a = 0.171 \pm 0.02$). Error bars of $\pm 20\%$ are included on the retrieved τ_a values (approximately twice that for the 17 July, 21 GMT retrieval) to include this and allow for S_a perhaps having some variability over the observed period. It can be seen that τ_a tended to remain fairly constant for a good 11 h extending from 16 July, 20 GMT to 17 July, 06 GMT. The observed descent of the dust layer (discussed earlier in connection with Fig. 1) did not appear to significantly impact the overall value of τ_a. The largest retrieved τ_a values occurred between 16–18 GMT

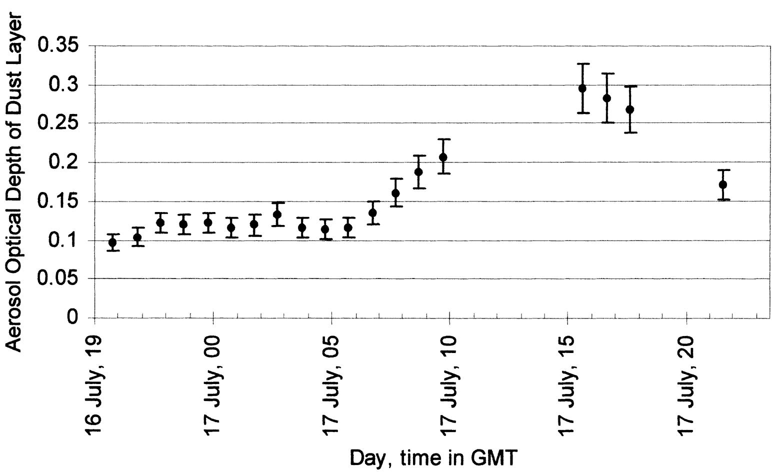

Fig. 3. Aerosol optical depth of dust layer retrieved using 2-scatter approach for time period 16 July, 20 GMT to 17 July, 22 GMT.

on 17 July. Fig. 4 displays profiles of $\sigma_a(z)$ and the $\tau_a(z)$ (aerosol optical thickness from the surface to height (z) for 16 and 18 GMT. Concurrent measurements were made at 16 GMT by an airborne sunphotometer (Schmid et al., 2000) to the south of Las Galletas. The sunphotometer measurements for 499 nm yielded $\tau_a = 0.24$ for the dust layer between 1 and 4 km, and $\tau_a = 0.05$ for the MBL below 1 km. Las Galletas MPL measurements were within 0.01 agreement of these values, obtaining $\tau_a = 0.25$ and, $\tau_a = 0.06$ for the respective regions. A comparison of $\sigma_a(z)$ for the dust layer also shows the two instruments to be in very good agreement, both yielding a peak value of $\sigma_a(z) \approx 0.17\ \mathrm{km}^{-1}$ at an altitude of approximately 3 km. A second opportunity for an instrument comparison was the 17 July, 18–19 GMT time period. Measurements from a second MPL (Welton et al., 2000) were taken at Izana Tenerife, a mountain top location north of Las Galletas. Measurements from the Izana MPL provided a value of $\tau_a = 0.177$ for the dust layer between approximately 2.4 and 4 km above MSL. Although Las Galletas is quite some distance from Izana (approximately 40 km north–northeast) it does seem meaningful that the Las Galletas MPL obtained a similar value of $\tau_a = 0.180$, an agreement within 0.003. This could suggest the dust layer was somewhat homogenous to the north and south.

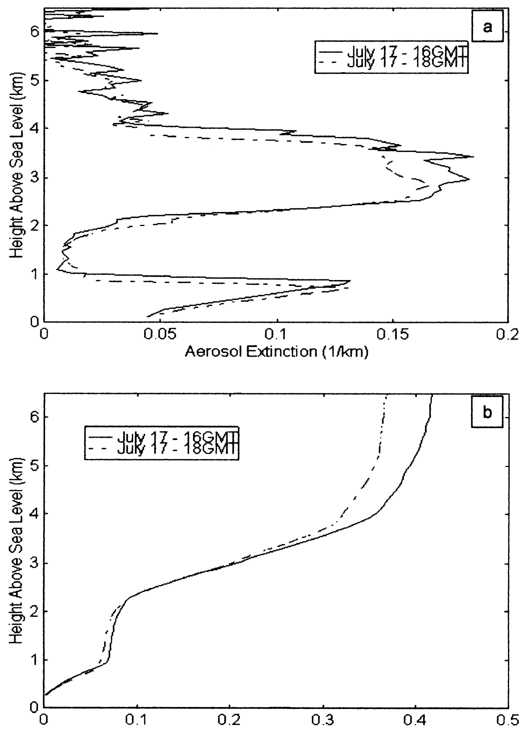

Fig. 4. Two-scatterer retrieval of aerosol extinction (a) and aerosol optical thickness (b) from vertical measurements 17 July, 16 and 18 GMT.

4.2. *Horizontal retrieval*

Taking advantage of the fact that atmospheric aerosols tend to be fairly homogeneously distributed in the horizontal, extinction $\sigma(r)$ can be retrieved from horizontal MPL measurements (Collis et al., 1966). For r along the horizontal, and homogeneous or constant σ, $T^2(r) = \exp(-2r\sigma)$, and a plot of $\ln[X(r)]$ versus $2r$ yields a straight-line of slope $-\sigma$. The aerosol component σ_a can be obtained by subtracting the known Rayleigh component. Typically the slope $-\sigma$ is obtained from the fit of a region selected between a range of 5 to 15 km. The scatter of points around the straight-line fit reflects how well the horizontal homogeneity assumption is met. An example of a straight-line fit from a horizontal measurement taken on 29 June at 20 GMT is illustrated in Fig. 5. The standard deviation of the fit gives a measure of uncertainty for the retrieved σ value. The horizontal retrieval technique is also useful for determining overlap. If the straight-line slope of $-\sigma$ is extended over the region affected by overlap, the overlap factor is given as the ratio of the signal to the straight-line fit value.

The horizontal measurements made at Las Galletas profiled the atmospheric layer approximately 25 m above the surface of the ocean. A plot of the retrieved surface σ_a values obtained from numerous horizontal sensing runs from 24 June to 24 July is shown in Fig. 6a. Aerosol optical depth τ_a values for the same time period retrieved from the co-located solar radiometer are also shown in Fig. 6b. Error bars give the standard deviation of each σ_a and τ_a value. A comparison of the two figures exhibits a strong positive correlation between the MPL surface σ_a and the τ_a from the solar radiometer measurements. In Fig. 6a of particular interest are the dramatic increases in surface σ_a which occur centered on 9 July and late on 18 July. The 9 July peak corresponds with an anthropogenic pollution outbreak that was observed in the sub-tropical North-East Atlantic during ACE-2 (Raes et al., 2000; Verver et al., 2000). The pollution outbreak was proceeded by relatively clean maritime air which is also reflected in the surface aerosol extinction for late June early July (Fig. 6a). The 18 July peak corresponds with a similar pollution outbreak but additionally is subsequent to the passage of the 16 and 17 July dust layer. As mentioned previously, vertical MPL measurements made late on 18 July (Fig. 1b) displayed evidence of residual Saharan dust in the upper troposphere as well as on top of the MBL. The proximity of the dust to the MBL suggest that dust may have infiltrated to the surface, thereby contributing along with the pollution outbreak to the enhanced surface extinction observed on 18 July. Further support that the dust was descending towards the MBL is offered by the detection of dust in air samples taken at the surface of Izana, Tenerife during the 16 and 17 July dust event (Hal Maring, personal communication 1999).

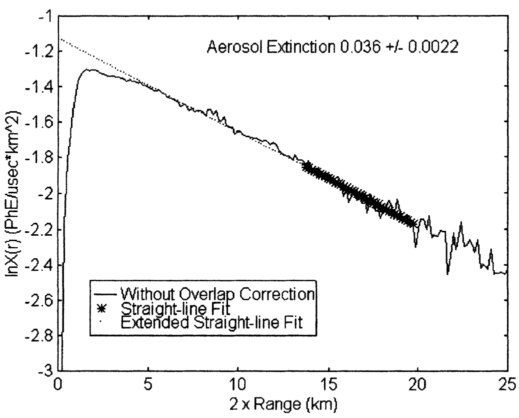

Fig. 5. Horizontal retrieval of aerosol extinction at the surface using slope method and fitting the range between 7 and 10 km. The normalized signal $X(r)$ is in units of $(\mathrm{PhE}/\mu)\,\mathrm{km}^2$.

5. Conclusion

The performance of the MPL during the ACE-2 campaign has demonstrated the system's ability to provide independent, quantitative aerosol optical properties based on the application of multiple angle measurements. In particular, values for τ_a retrieved from slant-sensing can replace the need for auxiliary measurements. Results obtained by combining established slant and vertical retrieval methods were in very good agreement with results obtained by a second MPL system and an airborne sunphotometer. Horizontal measurements, possible because of the eye-safe nature of the lidar system operated at Las Galletas, provided a sound quantitative optical and radiative representation of the dynamic state of atmo-

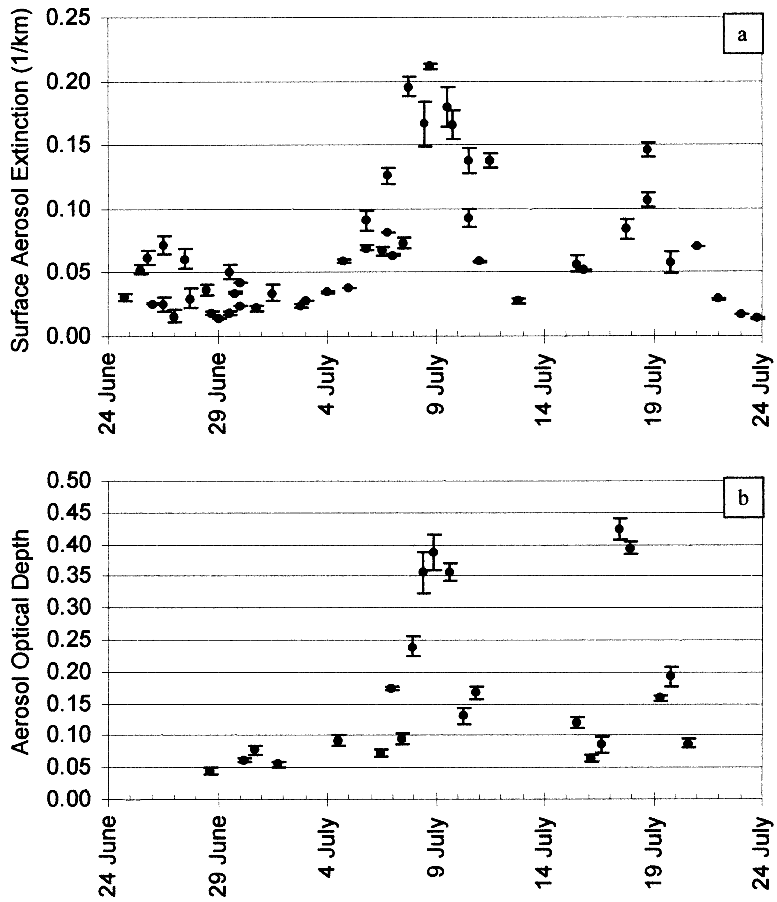

Fig. 6. Time Profile of surface aerosol extinction retrieved from horizontal MPL measurements (a) and aerosol optical depth retrieved from solar radiometer measurements (b) for 24 June to 27 July 1997. Error bars give the corresponding standard deviation of each value.

spheric aerosol at the surface. The MPL proved to be an effective and useful means for monitoring atmospheric phenomena such as Saharan dust events and anthropogenic pollution outbreaks. The near continuous operation of the system provided the opportunity to more thoroughly study the progression of the dust layer passage and the potential effects of dust events in the lower atmosphere and at the surface.

6. Acknowledgments

This work is supported by NSF under contract ATM9703609 and NASA Goddard Space Flight Center under contract NAG5-5105. The assistance and support from Hui Fang (University of Arizona) and James Campbell (Science Systems and Applications Inc.) has been greatly appreciated.

REFERENCES

Campbell, J. R., Hlavka, D. L., Spinhirne, J. D., Turner, D. D. and Flynn, C. J. 1998. Operational cloud boundary detection and analysis from micro pulse lidar data. *Proc. 8th ARM Science Team Meeting*. Tucson, AZ, pp. 119–122.

Collis, R. T. H. 1966. Lidar: a new atmospheric probe. *Quart. J. Roy. Meteorol. Soc.* **92**, 220–230.

Ehsani, A. R., Reagan, J. A. and Erxleben, W. H. 1998. Design and performance analysis of an automated 10-channel solar radiometer instrument. *J. Atmos. Oceanic Techn.* **15**, 200–210.

Fernald, F. G., Herman, B. M. and Reagan, J. A. 1972. Determination of aerosol height distribution by lidar. *J. Appl. Meterorol.* **11**, 482–489.

Karyampudi, V. M., Palm, S. P., Reagan, J. A., Fang, H., Grant, W. B., Hoff, R. M., Moulin, C., Pierce, H. F., Torres, O., Browell, E. V. and Melf, S. H. 1999. Validation of Saharan dust plume conceptual model using lidar, meteosat and ECMWF data. *Bull. Amer. Meteor. Soc.* **80**, 1045–1075.

Karyampudi, V. M. and Carlson, T. N. 1988. Analysis and numerical simulations of the Saharan air layer and its effects on easterly wave disturbances. *J. Atmos. Sci.* **45**, 3102–3136.

Powell, D. M., Reagan, J. A., Rubio, M. A., Erxleben, W. H. and Spinhirne, J. D. 1998. Micro-pulse lidar Tenerife, Canary Island Observations. *Proc. 8th ARM Science Team Meeting*. Tucson, AZ., 619–622.

Raes, F., Bates, T. S., McGovern, F. M. and Van Liedekerte, M. 2000. The second Aerosol Characterization Experiment (ACE-2): general overview and main results. *Tellus* **52B**, 111–126.

Reagan, J. A., Apte, M. V., Ben-David, A. and Herman, B. M. 1988. Assessment of aerosol extinction to backscatter ratio measurements made at 694.3 nm in Tuscon, Arizona. *Aerosol Science and Technology* **8**, 215–226.

Reagan, J. A., Apte, M. V., Bruhns, T. V. and Youngbluth, O. 1984. Lidar and balloon-borne csscase impactor measurements of aerosols: a case study. *Aerosol Sci. Technol.* **3**, 259–275.

Schmid, B., Livingston, J. M., Russell, P. B., Durkee, P. A., Jonsson, H. H., Collins, D. R., Flagan, R. C., Seinfeld, J. H., Gasso, S., Hegg, D. A., Ostrom, E., Noone, K. J., Welton, E. J., Voss, K. J., Gordon, H. R., Formenti, P. and Andreae, M. O. 2000. Clear sky closure studies of lower tropospheric aerosol and water vapor during ACE-2 using airborne sunphotometer, airborne in-situ, space-borne and ground-based measurements. *Tellus* **52B**, 568–593.

Spinhirne, J. D., Reagan, R. A. and Herman, B. M. 1980. Vertical distribution of aerosol extinction cross section and inference of aerosol imaginary index in the troposphere by lidar technique. *J. App. Meteorol.* **19**, 426–438.

Spinhirne, J. D. 1993. Micro pulse lidar. *IEEE Trans. Geosci. Remote Sensing* **31**, 48–55.

Spinhirne, J. D., Scott, V. S., Reagan, J. A. and Galbraith, A. 1995. Cirrus and aerosol lidar profilometer. *Proc. 5th ARM Science Team Meeting*. San Diego, CA., pp. 297–300.

Verver, G., Raes, F., Vogelezang, D. and Johnson, D. 2000. The second Aerosol Characterization Experiment (ACE-2): Meteorological and chemical context. *Tellus* **52B**, 126–140.

Welton, E. J., Voss, K. J., Gordon, H. R., Maring, H., Smirnov, A., Holben, B., Schmid, B., Livingston, J. M., Russell, P. B., Durkee, P. A., Formenti, P. and Andreae, M. O. 2000. Ground-based lidar measurements of aerosols during ACE-2: instrument description, results, and comparison with other ground-based and airborne measurements. *Tellus* **52B**, 636–650.